JARO
Journal of the Association for Research in Otolaryngology

Research Article

Direct Recordings from the Auditory Cortex in a Cochlear Implant User

Kirill V. Nourski,[1] Christine P. Etler,[2] John F. Brugge,[1,4] Hiroyuki Oya,[1] Hiroto Kawasaki,[1] Richard A. Reale,[1,4] Paul J. Abbas,[2,3] Carolyn J. Brown,[2,3] and Matthew A. Howard III[1]

[1]*Department of Neurosurgery, The University of Iowa, Iowa City, IA 52242, USA*

[2]*Department of Otolaryngology—Head and Neck Surgery, The University of Iowa, Iowa City, IA 52242, USA*

[3]*Department of Communication Sciences and Disorders, The University of Iowa, Iowa City, IA 52242, USA*

[4]*Department of Psychology, University of Wisconsin—Madison, Madison, WI 53706, USA*

ABSTRACT

Electrical stimulation of the auditory nerve with a cochlear implant (CI) is the method of choice for treatment of severe-to-profound hearing loss. Understanding how the human auditory cortex responds to CI stimulation is important for advances in stimulation paradigms and rehabilitation strategies. In this study, auditory cortical responses to CI stimulation were recorded intracranially in a neurosurgical patient to examine directly the functional organization of the auditory cortex and compare the findings with those obtained in normal-hearing subjects. The subject was a bilateral CI user with a 20-year history of deafness and refractory epilepsy. As part of the epilepsy treatment, a subdural grid electrode was implanted over the left temporal lobe. Pure tones, click trains, sinusoidal amplitude-modulated noise, and speech were presented via the auxiliary input of the right CI speech processor. Additional experiments were conducted with bilateral CI stimulation. Auditory event-related changes in cortical activity, characterized by the averaged evoked potential and event-related band power, were localized to posterolateral superior temporal gyrus. Responses were stable across recording sessions and were abolished under general anesthesia. Response latency decreased and magnitude increased with increasing stimulus level. More apical intracochlear stimulation yielded the largest responses. Cortical evoked potentials were phase-locked to the temporal modulations of periodic stimuli and speech utterances. Bilateral electrical stimulation resulted in minimal artifact contamination. This study demonstrates the feasibility of intracranial electrophysiological recordings of responses to CI stimulation in a human subject, shows that cortical response properties may be similar to those obtained in normal-hearing individuals, and provides a basis for future comparisons with extracranial recordings.

Keywords: averaged evoked potential, cortical plasticity, electrical stimulation, electrocorticography, high gamma, intracranial electrophysiology

INTRODUCTION

Hearing loss is a major public health problem, and electrical stimulation of the auditory nerve with a cochlear implant (CI) is the therapeutic option of choice for cases of severe-to-profound sensorineural hearing loss (NIH 1995). In a CI, an array of electrodes implanted in the cochlea restores the sense of hearing by directly stimulating fibers of the auditory nerve. CIs have been in clinical use since the early 1980s, with more than 219,000 devices implanted worldwide (NIDCD 2011). Development of novel electrode designs, stimulation paradigms, and surgical techniques over the years has contributed to the "modern miracle" of hearing restoration with

Correspondence to: Kirill V. Nourski • Department of Neurosurgery • The University of Iowa • 200 Hawkins Dr. 1815 JCP, Iowa City, IA 52242, USA. Telephone: +1-319-3357049; fax: +1-319-3536605; email: kirill-nourski@uiowa.edu

CIs (Ashley 2000), which can provide users with a high degree of speech perception accuracy (Krueger et al. 2008).

Central auditory processing plays a critical role in the utilization of auditory information provided by the CI (Moore and Shannon 2009). Studies in experimental animals and in human subjects provide evidence for improvements in CI performance over the weeks and months following implantation (Fallon et al. 2009). These improvements are thought to parallel changes in auditory cortex functional organization, suggesting that plasticity in the auditory cortex may play a role in this enhanced performance (Klinke et al. 1999, 2001; Giraud et al. 2001; Irvine et al. 2006; Kral and Tillein 2006). In order to further improve the design of CIs and refine post-implantation rehabilitation strategies, it is important to gain a better understanding of how the human auditory cortex responds to stimulation by these devices.

Research performed in our laboratory employs direct intracranial recording in neurosurgical patients to study the functional organization of the human auditory cortex. This method provides an opportunity to study the human auditory cortex with high spatial and temporal resolution (Engel et al. 2005; Cervenka et al. 2011; Howard et al. 2012). We have previously described an acoustically responsive area on the posterolateral portion of the superior temporal gyrus (STG), functionally distinct from primary and primary-like auditory cortex of Heschl's gyrus (Howard et al. 2000). We refer to this area as the posterolateral superior temporal auditory area (PLST). This area, which may comprise more than one functional field, responds robustly to a wide range of stimuli, including pure tones, trains of acoustic clicks, modulated noise bursts, and speech utterances (Reale et al. 2007; Brugge et al. 2008b; Nourski et al. 2010; Greenlee et al. 2011; Nourski et al. 2013a, b).

The current study presents the first case of direct recordings from the auditory cortex in a bilateral CI user. The patient had medically intractable epilepsy and underwent intracranial electrode implantation as part of her epilepsy surgery treatment plan. This provided a unique opportunity to examine directly the functional organization of the human auditory cortex in a deaf subject with CIs and to compare these findings with those of normal-hearing neurosurgery patients who were studied using comparable stimulus paradigms and intracranial recording methods.

Noninvasive recording of cortical averaged evoked potentials (AEPs) using scalp electroencephalography (EEG) in CI users has proven to be technically difficult. CI stimulation generates an electrical artifact that interferes with identification of the AEP, often requiring application of specialized artifact rejection strategies (Singh et al. 2004; Gilley et al. 2006; Martin 2007; Brown et al. 2008; Viola et al. 2012). In contrast, recording directly from the cortical surface has the advantage of yielding highly localized responses with a relatively high signal-to-noise ratio. In this study, we determined that it was possible to record responses to CI stimulation directly from the brain and that the stimulus artifact was a relatively minor factor in the recording.

The major goal of this study was to compare activity elicited on the posterolateral surface of the STG by electrical stimulation of the CI with that observed in normal-hearing subjects in response to acoustic stimuli. Most processing strategies used in CIs are based on extraction and accurate representation of temporal envelope information. In contrast, the amount of spectral information provided to the auditory system is limited due to the relatively small number of independent CI stimulation channels (Shannon 2007; Wilson and Dorman 2009). Temporal processing abilities in CI users have been shown to strongly correlate with speech recognition performance (Fu 2002). Therefore, we used a range of periodic and amplitude-modulated stimuli to focus on cortical representation of temporal sound features, for which we have previously recorded responses from PLST in normal-hearing listeners (Nourski et al. 2008, 2010, 2013a).

Additionally, we used time-compressed (accelerated) speech sentences. Previous studies in normal-hearing listeners have demonstrated that time compression of speech led to decreases in intelligibility and in phase locking of the auditory cortical responses to the temporal envelopes of these sentences (Ahissar et al. 2001; Ahissar and Ahissar 2005). Our previous studies have used these stimuli to establish that time locking to the speech temporal envelope could be present in core auditory cortex even when speech was severely time-compressed and, as a result, incomprehensible (compression ratio 0.20). In contrast, time locking of responses recorded from PLST was limited to moderately compressed speech (compression ratios 0.75–0.40) (Nourski et al. 2008, 2009). Accordingly, we used these stimuli to tax the temporal processing mechanisms in a controlled manner and to compare the brain responses recorded in the CI user to those obtained in subjects with normal hearing.

Portions of this study have appeared previously in abstract form (Nourski et al. 2012). Two companion studies have investigated cortical responses to self-vocalization and audiovisual speech in the same subject (Greenlee et al. 2012; Rhone et al. 2012).

METHODS

Subject

The subject was a 58-year-old female with 20 years of experiencing CI use. She had a history of toxic shock syndrome with coma in 1991 at the age of 38. She was treated with ototoxic antibiotics, which resulted in profound bilateral sensorineural hearing loss. Audiometric testing conducted a few months prior to placement of her first (right) CI showed relatively flat thresholds, above 90 dB HL, bilaterally. A 3-month hearing aid trial provided no benefit. Word recognition testing conducted at the time resulted in scores of 0 % on all of the following tests: spondee recognition, Northwestern University #6 words (Tillman and Carhart 1966), and Central Institute of the Deaf sentences (Hirsh et al. 1952).

This subject received an eight-channel Clarion C1 CI in her right ear in 1992, 14 months after she lost her hearing. In 2006, she received an Advanced Bionics HiRes 90K CI with 16 intracochlear contacts in her left ear. Both implant surgeries were performed at the University of Iowa Hospitals and Clinics. The surgeries were without complications, and full electrode insertions were obtained in both cochleae.

Both CIs were programmed to operate in monopolar stimulation mode. The right ear was fit with a Harmony BTE processor loaded with a seven-channel continuous interleaved sampling program (406 pulses/s per channel rate, 150 μs pulse duration). Channel 3 was found to be defective and was disabled. For clarity of presentation in this paper, intracochlear stimulation sites are referred to by numbers, while cortical recording sites are referred to by upper case letters. The left ear was fit with an Auria BTE processor loaded with a 14-channel HiRes-P program (3,458 pulses/s per channel rate, 21 μs pulse duration).

At the time of the experiments, the subject had been using the right ear CI for 20 years and bilateral CIs for 6 years. The subject has been using the same speech processor in the right ear for the last 2 years and the same processing strategy for over 6 years. In the left ear, she has been using the same speech processor and processing strategy since they were activated 6 years ago. The patient reported that she received benefit from both devices. She achieved a total score of 22 on the Hearing Handicap Inventory for the Elderly, corresponding to a mild emotional and situational hearing handicap (Ventry and Weinstein 1982). At the time of testing, the subject's consonant-nucleus-consonant monosyllabic words scores were 66 % phonemes correct and 39 % words correct for the right ear, 60 % phonemes and 31 % words correct for the left ear, and 73 % phonemes and 51 % words correct when tested in the binaural

listening mode. Her binaural City University of New York sentence score (Boothroyd et al. 1985) was 72 %. The subject was also assessed using the Hearing in Noise Test sentences (Nilsson et al. 1994) presented to the right ear only and received scores of 95 % correct in quiet and 85 % correct when testing was conducted in noise. Neuropsychological evaluation indicated strong left-handedness. Intracarotid amytal (Wada) test indicated left hemisphere language dominance and right-lateralized anterograde memory function.

We chose to carry out the majority of the experiments with the subject using the CI in her right ear and the speech processing program she used for everyday listening. Intracranial recordings were made from the left hemisphere in this subject (see below). We chose to focus attention on contralateral CI stimulation thinking that this would result in the strongest cortical excitation patterns and that the electrical pulses generated by the contralateral CI would be less likely to interfere with the intracranial recordings.

The subject developed medically intractable epilepsy subsequent to her hearing loss. As part of her diagnostic and treatment plan for refractory epilepsy, she underwent a short-term (3-day) intracranial electrode implantation over the left temporal lobe. The intracranial electrode grid was implanted for the purpose of electrical stimulation mapping of language areas on the left temporal lobe to spare areas critically involved in language function during resection surgery. The seizure focus was localized to the left mesial temporal lobe, and none of the acoustically responsive cortical sites on the lateral surface of the STG exhibited evidence of epileptic activity.

Click train-evoked AEP latencies obtained from the CI user were compared to those obtained under the same stimulus conditions from a group of ten normal-hearing neurosurgical patients (three females and seven males, between 28 and 47 years old). Auditory cortical responses obtained in these control subjects have been presented in earlier reports from our group (Brugge et al. 2009; Nourski et al. 2013a).

Stimulation

Experimental auditory stimuli were delivered to the CI speech processors through the auxiliary input. The majority of the experiments detailed in this report were carried out using stimulation of the right ear CI only, i.e., contralateral to the hemisphere onto which the recording grid was placed. In order to focus on a narrow region of the tonotopically organized cochlea, single-channel stimulation was carried out by driving custom speech processor programs with pure tone bursts (duration 300 ms, 5 ms on/off ramp). The

tones matched the center frequencies of the pass-band of the target CI channels on the right side. Each CI channel was stimulated for a total of 100 trials.

A variety of other stimuli were employed using the patient's everyday clinical program. Previous work in our laboratory has involved recording electrocortigographic (ECoG) responses to the same stimuli delivered acoustically in normal-hearing neurosurgery patients implanted with intracranial electrodes. These stimuli included click trains (Brugge et al. 2009; Nourski et al. 2013a), sinusoidally amplitude-modulated (SAM) noise bursts (Brugge et al. 2008a; Nourski et al. 2010), and time-compressed speech sentences (Nourski et al. 2008, 2009). Click train stimuli were generated digitally as equally spaced rectangular pulses (0.2 ms duration). SAM noise stimuli were generated by modulating a Gaussian noise burst carrier with sinusoids. Click trains and SAM noise bursts were presented at rates of 4, 8, 16, 32, 50, and 100 Hz (duration 1 s). Stimuli of the six rates were each presented 50 times in random order. These stimuli were presented in a passive listening paradigm, without any task direction.

Speech sentences, digitized at a sampling rate of 24,414 Hz, were time-compressed to ratios between 0.75 and 0.20 of the natural speaking rate using an algorithm that preserved the spectral content of the stimuli, as implemented in Sound Designer II software (Digidesign, Daly City, CA, USA). The experimental protocol employed a set of six time-compressed speech stimuli: five of the stimuli were time-compressed versions of a sentence "Black cars cannot park," presented at compression ratios of 0.75, 0.50, 0.40, 0.30, and 0.20. The sixth stimulus, "Black dogs can all bark," presented at a compression ratio of 0.75, was used as a target in an oddball detection task designed to maintain the subject in an alert state and evaluate comprehension of the sentences in the least compressed condition. The subject was instructed to press a button whenever the oddball stimulus was detected. The duration of the speech stimuli ranged from 0.29 to 1.05 s (at compression ratios of 0.20 and 0.75, respectively). This protocol was run twice, once with contralateral CI stimulation and once with simultaneous stimulation of both CIs.

The interstimulus interval in all experiments was chosen randomly within a Gaussian distribution to reduce stimulus predictability and to allow more efficient AEP estimation. The mean onset-to-onset interval was 2 s for single-channel pulse trains, click trains, and SAM noise, and 3 s for speech sentences; standard deviation was 10 ms for all stimuli. Stimuli were presented at a level that the subject judged to be comfortably loud. Stimulus delivery and data acquisition were controlled by a TDT RZ2 real-time processor (Tucker-Davis Technologies, Alachua, FL, USA).

Previously, we showed that the AEP recorded from posterolateral STG was abolished by general anesthesia (Howard et al. 2000). A similar opportunity arose to obtain recordings from the CI subject in the operating room before and after induction of general anesthesia with propofol (100 μg/kg/min, i.v.). For this purpose, we used 300 ms electric pulse trains delivered to channel 1 of the contralateral CI using a custom speech processor program and 50 Hz click trains (duration 500 ms) presented using the patient's everyday clinical program of the contralateral CI.

Response recording

ECoG recordings were obtained from a multicontact subdural grid electrode (AdTech, Racine, WI, USA) implanted over the lateral surface of the left temporal lobe (Fig. 1). The recording array consisted of platinum–iridium disc electrodes (2.3 mm exposed diameter, 5 mm interelectrode distance), embedded in a silicon membrane. The electrodes were arranged in an 8×12 grid, yielding a 3.5×5.5-cm array of 96 contacts. The electrode grid was placed solely on the basis of clinical requirements. The electrical potential obtained at each recording contact was referenced to a subgaleal electrode placed under the scalp in the left posterior frontal area of the skull.

Presence of bilateral CIs in this subject precluded a pre-implantation structural magnetic resonance imaging (MRI) study and limited the exposure and visualization of the brain surface during the surgery to a relatively small craniotomy (Fig. 1A). Anatomical location of the recording sites was determined using co-registration of post-implantation and post-resection high-resolution computed tomography (CT) scans with a template brain volume, aided by intraoperative photography. Two high-resolution postoperative CT scans (0.59×0.59 mm in-plane resolution, 1.0 mm slice thickness) were obtained postoperatively, one the day after recording electrode implantation and the other one the day after recording electrode removal and seizure focus resection. The two CT scans were co-registered using a six-parameter linear transformation (rigid co-registration) (Fig. 1B). Recording contacts were identified in the post-implantation CT scan and transferred onto a template ICBM152 average brain (average of 152 normal MRI scans in the Montreal Neurological Institute space) (Fig. 1C). Post-resection CT volume and the ICBM152 volume were first co-registered using a linear Affine transformation, followed by a nonlinear morphing of the CT volume onto the MRI template volume using symmetric diffeomorphic mapping (Avants et al. 2006, 2008). Both mutual information and point set matching were used for the mapping procedure.
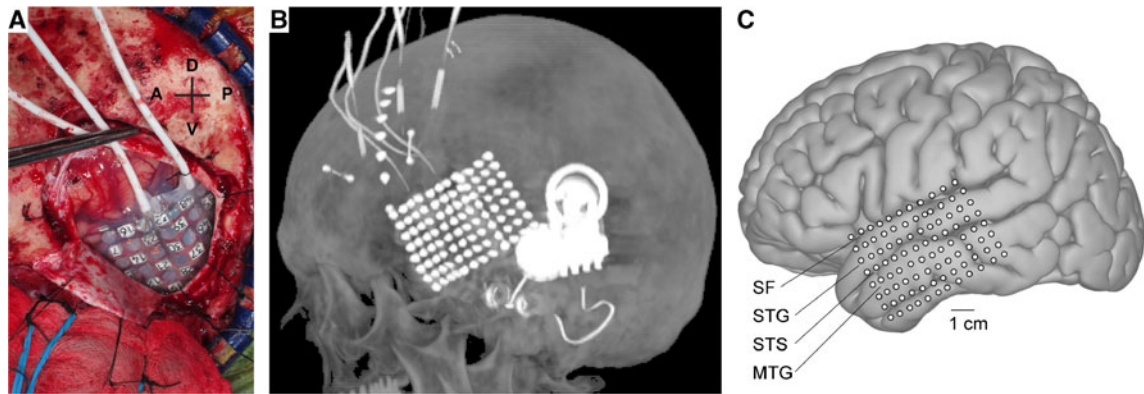
FIG. 1. Placement of the recording grid electrode. **A** Intraoperative photo. **B** 3D reconstruction of the post-implantation CT scan. **C** Projection of the contact location onto ICBM152 template brain. *SF* sylvian fissure, *STG* superior temporal gyrus, *STS* superior temporal sulcus, *MTG* middle temporal gyrus.

Data analysis

ECoG data obtained from each recording site were analyzed as the AEP and, in the time–frequency plane, as event-related band power (ERBP) (reviewed by Cervenka et al. 2011). Data analysis was performed using custom software written in the MATLAB Version 7.13.0 programming environment (MathWorks, Natick, MA, USA).

Pre-processing of ECoG data included downsampling to 1 kHz for computational efficiency, followed by removal of power line noise (60 Hz and its harmonics) by an adaptive notch filtering procedure (Nourski et al. 2013a). Additionally, single-trial (peri-stimulus) ECoG waveforms with voltage peaks or troughs greater than 2.5 standard deviations from the mean were eliminated from the data set prior to further analysis. This would include activity generated by electrical interference, epileptiform spikes, high-amplitude slow-wave activity, or movement artifacts.

ECoG data recorded in response to contralateral CI stimulation and pre-processed as described above were essentially free from electrical stimulus artifact. The proximity of the ipsilateral CI to the recording electrode resulted in an electric stimulus artifact evident in ECoG recordings obtained during bilateral CI stimulation. To minimize the artifact that could potentially obscure physiological responses, single-trial waveforms from the 96 recording sites in this stimulus configuration were transformed with a spatial filter using the surface Laplacian operation (Nunez 1981; Nunez and Pilgreen 1991; Reale et al. 2007). The surface Laplacian is independent of the reference electrode and ameliorates the effects of spatial smearing of ECoG voltage due to volume conduction in the tissue and fluid of the brain. The surface Laplacian required an accurate representation of the spatial distribution of potential, which was derived using spline interpolation (Perrin et al. 1987; Law et

al. 1993). This results in a close correspondence between pre- and post-transformation waveforms, particularly at recording sites that are the closest to the foci of cortical activity (Reale et al. 2007).

The latency of each of the four prominent peaks (P_α, N_α, P_β, and N_β) and the N_α–P_β peak-to-peak amplitude of the AEP were measured (Howard et al. 2000). AEP peak latencies of responses to 100 Hz click trains obtained in the CI user were compared with latencies measured in response to the same stimulus waveforms presented acoustically in ten normal-hearing subjects, studied previously (Brugge et al. 2009; Nourski et al. 2013a). The frequency-following response (FFR) to repetitive stimuli (click trains and SAM noise bursts) was visualized by high-pass filtering the AEP waveforms with a cutoff frequency of 1 octave below the stimulus repetition rate.

Time–frequency analysis of the ECoG was performed using wavelet transforms based on complex Morlet wavelets following the approach of Oya et al. (2002). Center frequencies ranged from 20 to 200 Hz in 5 Hz increments. ERBP was calculated for each center frequency on a trial-by-trial basis and normalized to median baseline power, measured for the same center frequency within a window of 100 to 200 ms prior to stimulus onset. ERBP values were then log-transformed and averaged across trials.

For quantitative analysis of ERBP, we focused on the high gamma ECoG frequency band (Crone et al. 2001; Brugge et al. 2009; Edwards et al. 2009), which was defined in the present study within a range of center frequencies between 70 and 150 Hz. The wavelet constant ratio used for time–frequency analysis was defined as $f_0/\sigma_f=9$, where f_0 is the center frequency of the wavelet and σ_f is its standard deviation in frequency. Contribution of energy from post-stimulus onset interval to the estimate of baseline power was negligible for the

range of center frequencies analyzed. The magnitude of high gamma response was quantified by averaging high gamma ERBP within the time window of 50–250 ms after stimulus onset.

Representation of the temporal stimulus envelope in the cortical activity was quantified in the time domain using cross-correlation analysis (Ahissar et al. 2001; Abrams et al. 2008; Nourski et al. 2009). Envelopes of the speech stimuli were obtained by calculating the magnitude of the Hilbert transform of the speech signal waveform and low-pass filtering at 50 Hz using a fourth-order Butterworth filter. Peaks of cross-correlograms between the stimulus envelope and the cortical response (AEP waveform and high gamma ERBP) were found between lags of 0 and 150 ms. Following the approach of Millman et al. (2013), stimulus–response cross-correlation in the time domain was evaluated using a bootstrap procedure to generate surrogate data, followed by an approximate permutation test that provided the estimated P values and critical thresholds (Nichols and Holmes 2002). A surrogate data set was generated from the original single-trial ECoG waveforms by selecting, at random, half of the trials and inverting their waveforms. The measured peak of the cross-correlogram between the stimulus envelope and the surrogate AEP provided a value of the statistic that would be expected to occur by chance. The permutation distribution of this statistic under the null hypothesis (i.e., no correlation between the stimulus and the response) was obtained by generating 5,000 surrogate data sets and measuring the peaks in their resulting cross-correlograms. The null hypothesis was rejected when the peak of cross-correlogram between the stimulus envelope and the original AEP was greater than the $100(1 - \alpha)$th percentile ($\alpha = 0.05$) of the permutation distribution. Similarly, significance of cross-correlation between the stimulus envelope and high gamma ERBP response was evaluated by constructing surrogate data sets ($n = 5,000$) from single-trial high gamma ERBP waveforms and using the 95th percentile of the permutation distribution as the threshold criterion.

RESULTS

Responses to single-channel pulse trains

We characterized ECoG responses to electric pulse trains presented on single stimulation channels of CI using custom programs for the speech processor on the right (contralateral) ear. Pitch ranking conducted during programming of the CI speech processor revealed all functional channels (1 through 8, except channel 3) to be in the correct order, from low to high. Responses elicited by

stimulation on the most apical electrode (i.e., channel 1) are presented in Figure 2. In this figure, placement of the recording grid is shown along with exemplary AEP and ERBP data from four different recording sites (Fig. 2A) and the entire recording grid (Fig. 2B). The strongest cortical responses were obtained from the most posterior recording sites on the STG. AEPs and ERBP obtained by CI stimulation were similar to those obtained from field PLST in response to acoustical stimulation. ERBP was maximal in the high gamma frequency range, and its spatial distribution across the cortical surface was more restricted compared to the AEP. One site (site A, Fig. 2) was characterized by both highest amplitude AEPs and largest high gamma ERBP in response to all stimuli used in this study. Other cortical sites exhibited different response patterns, including AEPs in the absence of high gamma ERBP (e.g., site B, Fig. 2), high gamma responses without AEP onset deflections (site C, Fig. 2), or showed neither AEP nor ERBP responses (site D, Fig. 2). Taken together, we interpret the obtained CI responses as most likely arising from the anterior portion of what we previously described as area PLST in normal-hearing subjects.

Previous work has demonstrated that AEPs recorded from PLST are stable over multiple recording sessions and are abolished under general anesthesia (Howard et al. 2000). Similar results were obtained from the CI subject. AEPs were collected in four different sessions over 2 days (Fig. 3A), followed by a recording session in the operating room before and after induction of general anesthesia (Fig. 3B). The stimulus was a 300-ms 406-Hz pulse train delivered on channel 1 of the right CI. Cortical responses were stable throughout the duration of the monitoring period in terms of their magnitude and waveform. AEPs were no longer in evidence shortly after induction of general anesthesia with propofol.

The effects of stimulus intensity and the intracochlear place of stimulation were examined by presenting electric pulses on different CI channels at different intensities. The intensity-related changes in magnitude and latency of the AEPs obtained in response to these stimuli from site A of Figure 2 are summarized in Figure 4. Intracochlear electrodes 1 and 8 were the most apical and the most basal, respectively, as shown schematically in Figure 4A. The latency of AEP peak N_{α} generally decreased with stimulus intensity, although these changes were not always systematic for all stimulation sites (Fig. 4B), and the same trends were seen in the other three prominent peaks of the AEP waveform (data not shown). The magnitude of cortical responses, measured as the peak-to-peak amplitude of the AEP waveform and average high gamma ERBP within the 50–250-ms post-stimulus interval (left and right panels in Fig. 4C, respectively), generally increased with stimulus intensity. The magnitude of cortical responses was also influenced
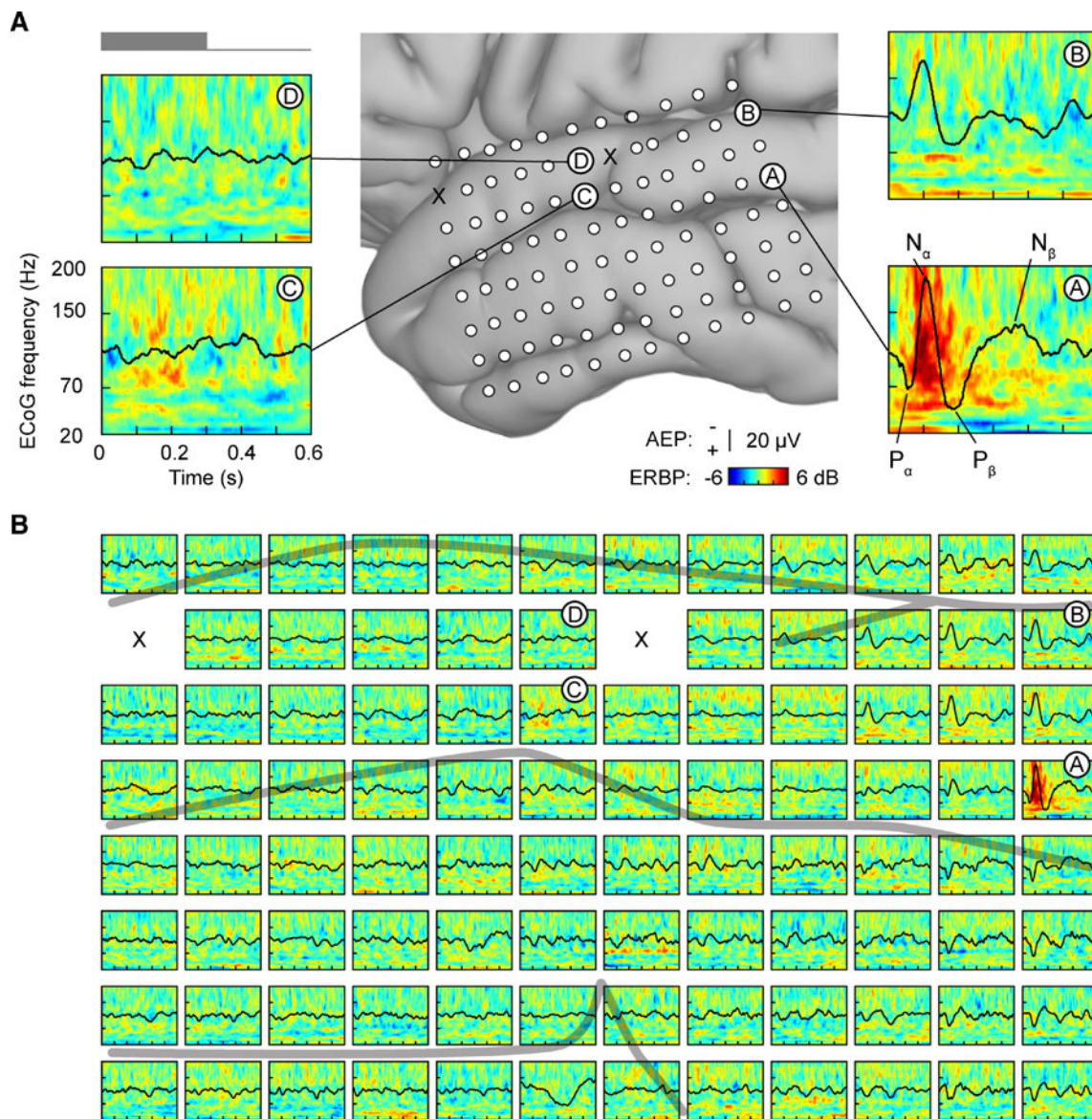
FIG. 2. Responses to 300 ms 406 Hz electric pulse trains, presented on channel 1 of the contralateral (right) CI. **A** AEP waveforms (*black lines*; negative voltage plotted upwards) and ERBP (*color plots*) recorded from four representative contacts on the STG (*A, B, C, D*, location shown in the center panel). The stimulus is schematically shown on the *top left in gray*. **B** AEPs and ERBP recorded from the whole grid. Defective contacts are marked with an "X." Cortical sulci are outlined by *thick gray lines*.

by the intracochlear location of the stimulus electrode; stimulation of more apical channels generally elicited larger cortical responses. We did not observe changes in the location of maximal cortical activity associated with the choice of intracochlear stimulation channel; cortical site A of Figure 2 featured the largest responses across the entire recording grid, regardless of intracochlear stimulus location and intensity.

Responses to click trains

Auditory cortical responses to repetitive acoustic stimuli, such as click trains or bursts of SAM, may be characterized in normal-hearing individuals by the AEP, the FFR, and ERBP (Brugge et al. 2009; Nourski and Brugge 2011; Nourski et al. 2013a). Figure 5 summarizes these cortical responses to trains of acoustic clicks presented via the CI. The stimuli were delivered through the auxiliary input using the clinical program of the right CI. Overall spatial activation patterns, shown in Figure 5A for 50 Hz click trains, were similar to those elicited by single-channel CI stimulation (see Fig. 2). The largest responses remained localized to the posterior edge of the recording grid (e.g., sites A, B), but in this case, responses could also be seen more anteriorly along the STG (e.g., site C).
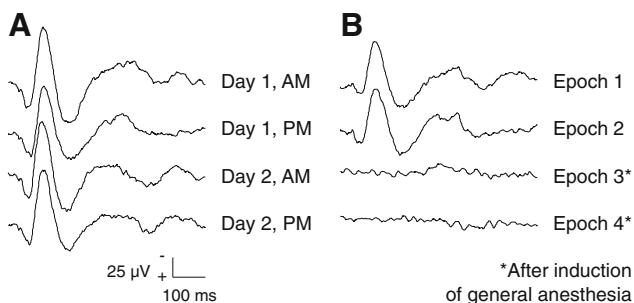
FIG. 3. Stability of electrically evoked cortical responses over time. AEPs recorded from site A (see Fig. 2A) in response to 300 ms 406 Hz electric pulse trains, presented on channel 1 of the contralateral (right) CI. **A** AEP morphology over four experimental sessions (2 days). **B** AEP morphology before and after induction of general anesthesia (*top two* and *bottom two traces*, respectively).

Latencies of the AEP waveform peaks P_α, N_α, P_β, and N_β from the maximally responsive site A were 73, 120, 223, and 366 ms, respectively, for the 100-Hz 1-s click train stimulus (Fig. 5B). AEP peak latencies measured in the CI user were not significantly different from those that characterized responses to the same click train stimulus in normal-hearing subjects. The latencies of all four peaks were within the 95 % confidence intervals of latencies measured in the normal-hearing control group ($N=10$), and the two negative peaks (N_α and N_β) were within the middle quartiles.

Detailed response properties of the four exemplary sites on the lateral STG are shown in Figure 5C for click rates between 4 and 100 Hz. As the pulse rate of individual stimulation channels on the right CI was 406 Hz, sparse sampling of the modulation envelope by the carrier pulse train (McKay et al. 1994) precluded analysis of responses to click trains of higher rates. Click train stimulation elicited robust responses characterized by AEP waveforms consistent with those previously ascribed to PLST in normal-hearing subjects (Howard et al. 2000; Reale et al. 2007; Nourski et al. 2013a) including onset and offset responses and growth in amplitude with increasing click rate.

Superimposed on the low-frequency AEP was an FFR. This response, emphasized for clarity in Figure 5C (red) by high-pass filtering the AEP waveforms with a cutoff frequency of 1 octave below the driving frequency, was evident at rates of up to 50 Hz on sites A and B. The FFR could also be observed for click rates of 32 and 50 Hz in the time–frequency plots as horizontal bands of ERBP at ECoG frequencies corresponding to the click rates (filled arrowheads in Fig. 5C). In contrast, there were no demonstrable phase-locked responses at the driving frequency of 100 Hz. Time–frequency analysis, however, revealed a subharmonic phase-locked component at 50 Hz in response to the 100-Hz click trains
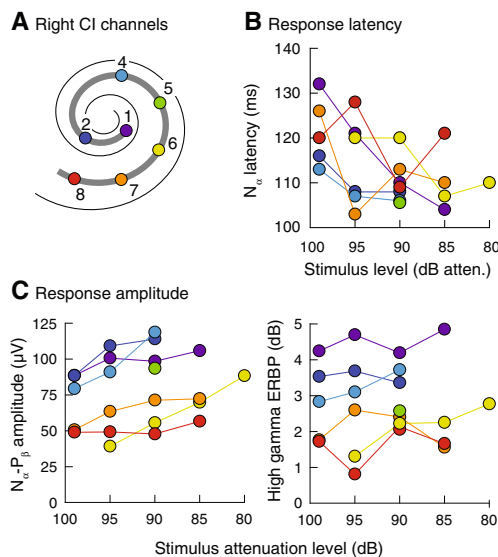

FIG. 4. Effects of stimulation site and stimulus intensity on the latency and amplitude of cortical responses recorded from site A. **A** Schematic of right CI electrode placement. **B** N_α peak latencies plotted as functions of stimulus level for different stimulation channels. **C** Peak-to-peak AEP amplitudes (*left panel*) and average high gamma ERBP, measured between 50 and 250 ms after stimulus onset (*right panel*), plotted as functions of stimulus intensity. Stimuli—300 ms 406 Hz electric pulse trains. *Different colors* in **B** and **C** represent different stimulation channels of the right CI, as depicted in **A**.

(open arrowhead Fig. 5B, site B). Overall, the capacity of the brain response to phase-lock to a periodic stimulus was comparable to that seen in normal-hearing subjects (Nourski et al. 2013a).

Click train stimuli also elicited ERBP changes in the high gamma frequency range. Similar to responses to single-channel CI stimulation, the spatial distribution of ERBP change was more restricted than that of AEPs. Comparison of time–frequency analysis of data recorded from sites A and B revealed a much more prominent high gamma response at site A.

An additional, more anterior, focus of cortical activity, exemplified in Figure 5C by sites C and D, was characterized by relatively long-latency and low-amplitude AEPs and absence of FFRs to any of the tested click rates. On the more responsive site C, ERBP was the largest in response to 100 Hz click trains and had a longer latency compared to more posterior sites A and B.

During the experiment performed in the operating room before and after induction of general anesthesia, 50 Hz 500 ms click trains were presented using the clinical program of the contralateral CI (Fig. 6). Recordings from two cortical sites A and B demonstrate that, prior to anesthesia and in the awake state, site A featured a larger amplitude AEP and a stronger high gamma response than site B, while site B was characterized
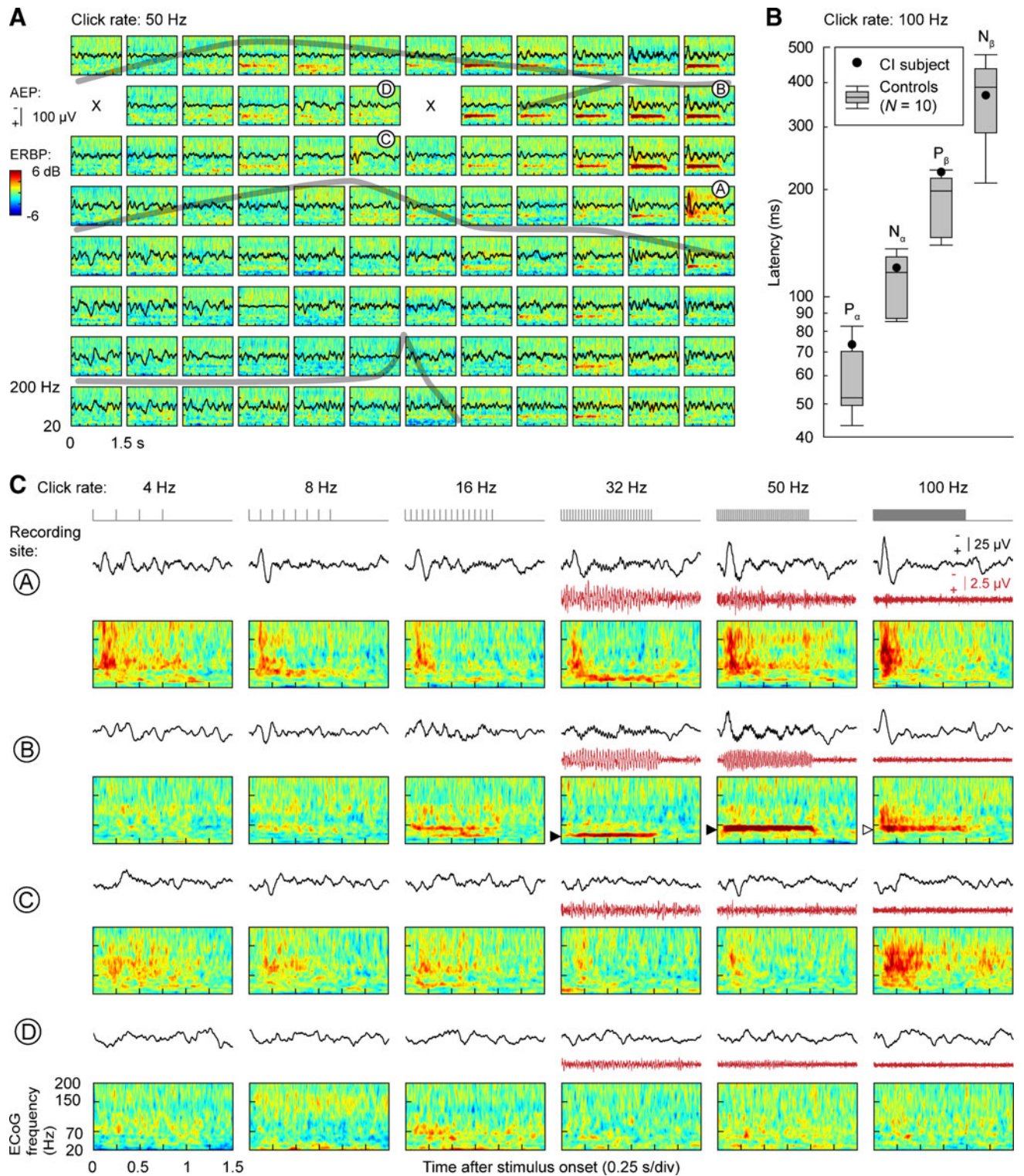
FIG. 5. Responses to click trains (duration 1 s), presented using the clinical program of the contralateral (right) CI. **A** AEPs (*black lines*) and ERBP (*color plots*) recorded from the whole grid in response to 50 Hz click trains. Defective contacts are marked with an "X." Cortical sulci are outlined by *thick gray lines*. **B** AEP peak latencies measured in response to 100 Hz click trains in the CI subject (*circles*) and ten normal-hearing subjects (*gray box plots*; median values, 25th and 75th percentiles, and 95 % confidence intervals are shown). **C** AEPs (*black lines*), FFRs (*red lines*), and ERBP (*color plots*), recorded from four representative contacts on PLST (*A–D*; *top* to *bottom*). *Filled* and *open arrowheads* indicate phase-locked responses to the driving frequency and its subharmonic, respectively. The stimuli are schematically shown on *top*.

by a stronger FFR (Fig. 6, left column). Following induction of general anesthesia, the AEP, the FFR, and ERBP were no longer in evidence, thus confirming and extending results obtained with single-channel CI stimulation (see Fig. 3).

Responses to SAM noise stimuli

SAM noise bursts, presented via auxiliary input of the contralateral CI using its clinical program, elicited responses at modulation rates between 4 and 100 Hz, as shown in Figure 7 for four representative cortical sites. Responses from sites A and B were time-locked to the temporal structure of the stimulus for rates of up to 50 Hz. At relatively low modulation rates (4–8 Hz), cortical locking to the stimulus envelope was evident in the unfiltered AEP waveforms, while at higher rates, activity phase-locked to the stimulus envelope was better revealed in the bandpass-filtered AEP waveforms. These patterns of cortical activity were similar to those observed in recordings from PLST in normal-hearing subjects (Nourski et al. 2010). Responses from more anterior portions of the grid (sites C and D in Fig. 7) were characterized by low-amplitude AEPs, absence of FFRs, and relatively small ERBP with longer latency compared to that recorded from sites A and B.

Responses to time-compressed speech

We examined cortical responses to time-compressed speech sentences "Black dogs cannot bark" and "Black cars cannot park," the same stimuli as used in our earlier studies (Nourski et al. 2008, 2009). The CI subject was instructed to press a button whenever she heard the target sentence "Black dogs cannot bark." During contralateral CI stimulation, the subject correctly identified all 50 trials of the target sentence and produced 11 "false alarm" responses to the nontarget sentence presented at a compression ratio of 0.75 and one "false alarm" response to the nontarget sentence compressed to a ratio of 0.50. All but one "false alarm" responses occurred within the first third (5 min) of the experimental session. When the protocol was repeated with bilateral CI stimulation, the subject correctly identified 48/50 trials of the target sentence and did not respond to any of the 250 nontarget stimuli.

Figure 8 presents analysis of cortical activity recorded from four sites in response to time-compressed speech sentences. Responses to both contralateral (Fig. 8A) and bilateral (Fig. 8B) CI stimulation were characterized by AEPs that tracked the temporal envelopes of moderately compressed sentences (compression ratios 0.75–0.40; sites A and B). Sustained ERBP responses reflected the overall duration of the
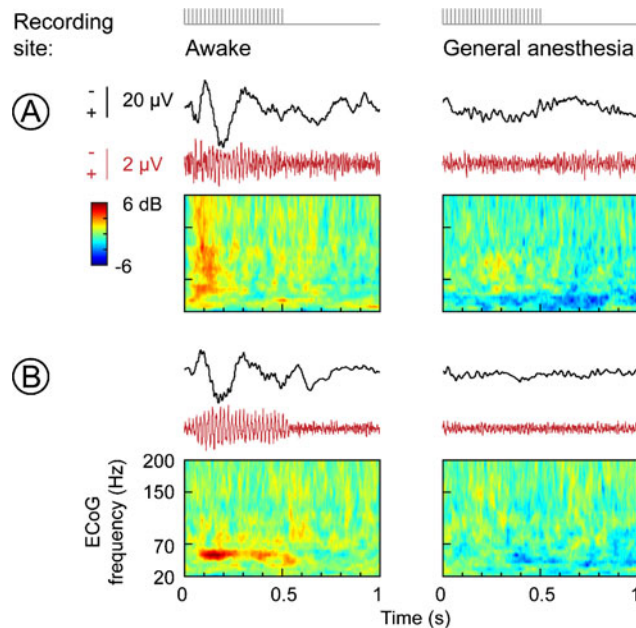

FIG. 6. Effects of general anesthesia on cortical AEP, FFR, and ERBP. Responses to 50 Hz click trains (duration 500 ms), recorded before and after induction of general anesthesia (*left* and *right* columns, respectively), are shown for two representative recording sites, A and B. The stimuli are schematically shown on *top*.

sentences yet did not appear to be modulated by their temporal envelopes. Site D, located relatively anterior on the recording grid and immediately dorsal to site C, yielded relatively strong responses to compressed speech compared to nonspeech stimuli (see Figs. 2, 5, and 7). No consistent differences were observed between responses to target and nontarget stimuli in terms of magnitude of the AEP or high gamma response. Bilateral electrical stimulation introduced a stimulus artifact (data not shown) which was minimized by applying a spline Laplacian transform to the data. Overall, responses from individual sites were comparable between contralateral and bilateral modes of stimulation.

Phase locking of the cortical response to the stimulus envelope at different compression ratios was quantified using cross-correlation analysis (Ahissar et al. 2001; Abrams et al. 2008; Nourski et al. 2009). Envelope following by the AEP and ERBP was measured as peaks of cross-correlograms between speech envelopes and AEPs and high-frequency ERBP envelope (70–150 Hz; see "Methods"), respectively. Figure 9 presents the results of this analysis performed on data obtained from four different sites. In more posterior sites A and B, correlation between the stimulus envelope and the AEP waveform envelope remained significant at moderate degrees of compression (0.75–0.40), but failed to reach significance at the two most compressed conditions (0.30–0.20). In contrast,
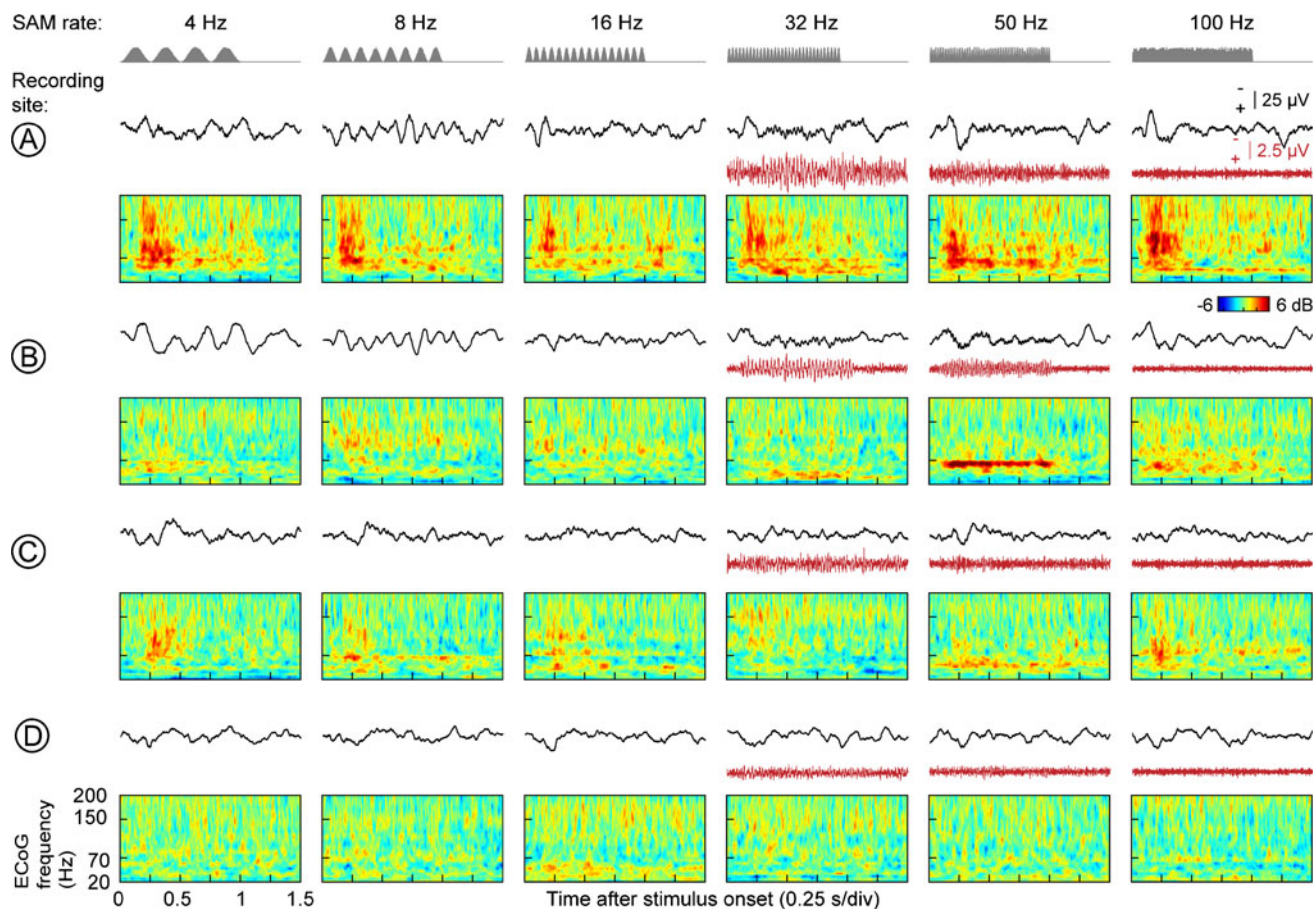
FIG. 7. Responses to 1-s bursts of SAM noise, delivered using the clinical program of the contralateral (right) CI. AEPs (*black lines*), FFRs (*red lines*), and ERBP (*color plots*), recorded from four representative contacts on PLST (*A–D*; *top* to *bottom*). Temporal envelopes of the stimuli are shown on the *top in gray*.

stimulus envelope following by high gamma ERBP was only found to be significant in the least compressed condition. Sites C and D, located more anteriorly along the STG, only featured significant correlations between stimulus envelope and the AEP in the least compressed stimulus conditions. Overall, there were no consistent differences in cross-correlation values between contralateral and bilateral stimulation conditions, or following of target vs. nontarget sentences presented at a compression ratio of 0.75.

DISCUSSION

To our knowledge, this is the first reported case where intracranial auditory cortical recordings were obtained in a deaf patient with cochlear implants. The direct recording method provided a unique opportunity to study the response properties of a relatively well-defined region of nonprimary auditory cortex (presumed PLST) resulting from electrical stimulation of the cochlea and compare these properties with those exhibited in normal-hearing subjects.

Area PLST in normal-hearing individuals is characterized by robust responses to a wide range of auditory stimuli and typically features one or more foci of maximal activity (Howard et al. 2000; Reale et al. 2007; Brugge et al. 2008b; Steinschneider et al. 2011; Nourski et al. 2013a, b). Spatial activation patterns on PLST elicited by pure tone stimuli typically vary as a function of stimulus frequency. Occasionally, an area is found representing low frequency separating areas representing higher frequency; typically, however, more complex and distributed patterns are seen (Nourski et al. 2013b). In the present study, changes in location of intracochlear stimulation were perceived by the subject (as determined by pitch ranking) but were not paralleled by changes in the spatial distribution of cortical activity. One cortical site was consistently most responsive to all the tested stimuli that were presented. This site was located on the posterior edge of the recording grid. The relatively anterior placement of the recording grid in this subject could have missed
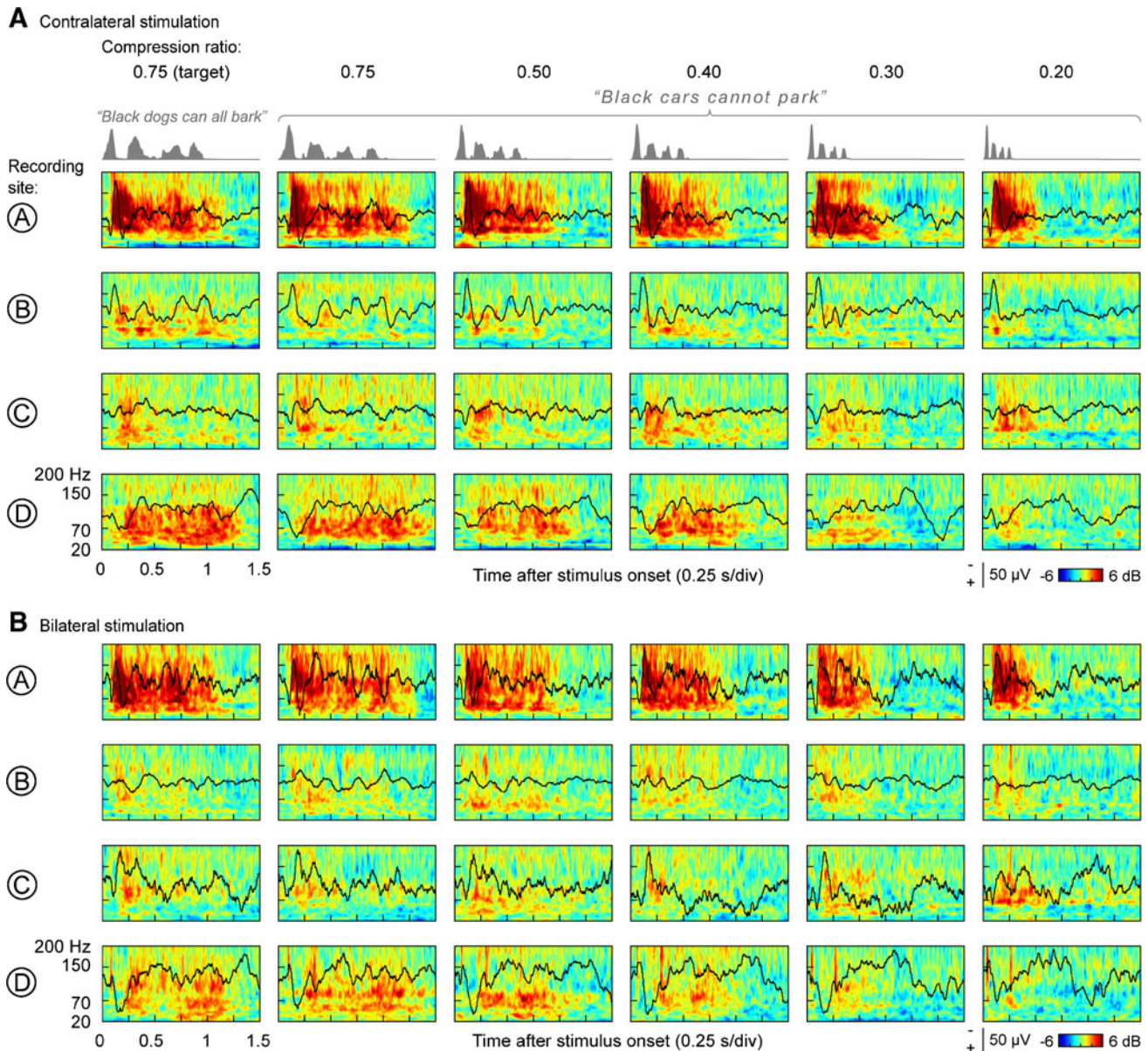
FIG. 8. Responses to time-compressed speech sentences "Black dogs can all bark" (*left column*) and "Black cars cannot park" (*all other columns*). AEPs (*black lines*) and ERBP (*color plots*), recorded from four representative contacts on PLST (*A–D; top* to *bottom*). *Left* to *right*: moderate to severe compression. Temporal envelopes of the stimuli are shown on the *top in gray*. **A** Responses to stimulation of the contralateral (right) CI. **B** Responses to bilateral CI stimulation.

much of area PLST located posteriorly and this could, at least in part, account for the observed lack of spatial distribution of cortical activity. In addition, the relatively poor spatial (electrodotopic) resolution of the CI may have contributed to the observed lack of effects in this subject.

In normal-hearing subjects, PLST often presents with topographically segregated response patterns, suggesting that this area may include multiple functional fields (Brugge et al. 2008b; Nourski et al. 2013b). In the present CI subject, an additional focus of activity, located more anteriorly along lateral STG,

was characterized by responses that varied significantly as a function of the type of stimulus delivered. This, along with the observation that high gamma activity recorded from anterior sites had longer onset latencies than that on more posterior sites, suggests that these foci of activity may correspond to two different functional fields identified in area PLST in normal-hearing subjects.

CI users have to rely heavily on temporal envelope information for speech perception, as the amount of spectral information (independent stimulation channels) provided by the implant is limited (Fu 2002;
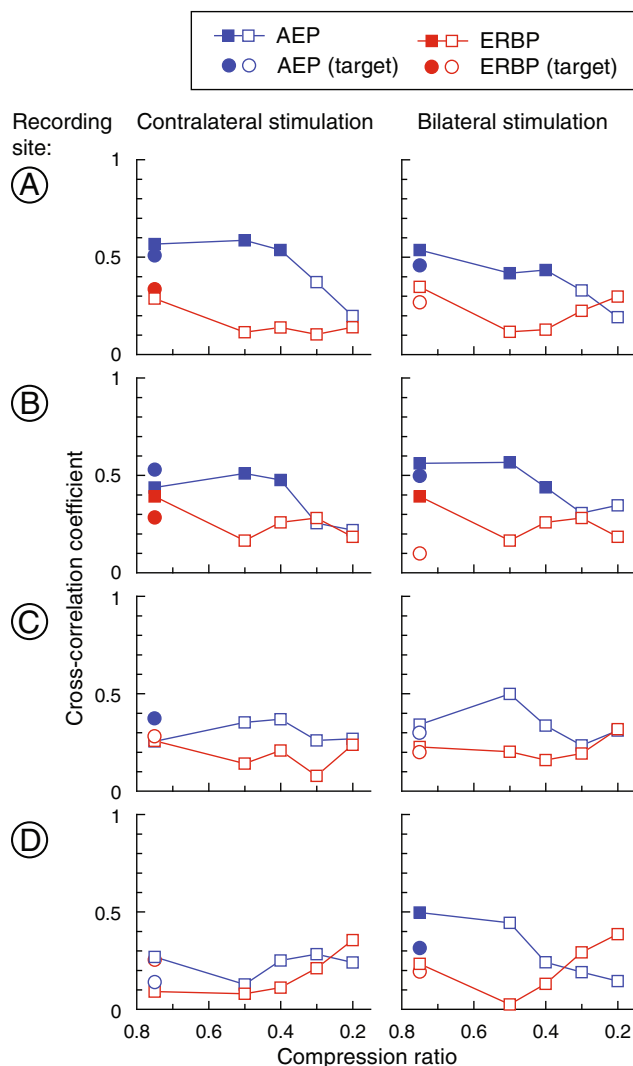
FIG. 9. Peak values of cross-correlograms between speech enve-lopes and AEPs (*blue*) and between speech envelopes and high gamma ERBP (*red*). *Circles* and *squares* represent responses to target and nontarget stimuli, respectively. Data from four representative contacts on PLST are shown (*A–D*; *top* to *bottom*). Significant (>95th percentile, permutation test) and nonsignificant values are shown by *filled* and *open symbols*, respectively. The data obtained using contralateral and bilateral CI stimulation are shown in the *left* and *right columns*, respectively.

recording grid could explain this finding. A subharmonic component at 50 Hz was detected in the time–frequency analysis of responses to 100 Hz click trains. This could be a result of aliasing, wherein the 100-Hz click trains used to modulate 406 Hz CI pulse train carriers produced a 50-Hz component at the output of the speech processor due to sparse sampling of the modulation envelope by the carrier (McKay et al. 1994).

AEPs elicited by time-compressed speech sentences were phase-locked to the temporal envelope of speech at moderate compression ratios (0.75–0.40). Clinical considerations limited the duration of experimental sessions and the amount of data that could be collected. This limit precluded a detailed psychophys-ical evaluation of the subject's comprehension of time-compressed speech. However, the subject could discriminate between the target and the nontarget sentence presented in the least compressed condition. Decline in temporal envelope tracking by the AEP with increasing speech compression in this subject paralleled changes in comprehension of such sentences by normal-hearing individuals reported previously (Nourski et al. 2009). This indicates that speech envelope information of stimuli presented within the intelligible range is preserved at the level of noncore cortex of PLST in this CI user. This is different from core auditory cortex, where temporal envelope following through modulation of high gamma activity could exceed perceptual capacity (Nourski et al. 2009), but is consistent with our observations from PLST obtained in normal-hearing subjects (Nourski et al. 2008).

This CI user had extensive (over 20 years) CI experience and good speech recognition perfor-mance. The CI user experienced many years of altered sensory input to the auditory cortex. Absence of neurotrophic support from hair cells and supporting cells to spiral ganglion neurons likely caused at least some degree of degeneration of the auditory nerve (Linthicum and Anderson 1991; Linthicum et al. 1991; Fayad and Linthicum 2006; Shepherd and Hardie 2001). Despite this, the overall waveform shape and peak latency of responses recorded from this nonprimary auditory cortex was similar to that observed in individuals with normal hearing.

AEPs derived from auditory cortical responses recorded with scalp EEG electrodes are generally characterized by a series of positive and negative peaks with latencies ranging from about 50 to 300 ms after stimulus onset (Näätänen and Picton 1987; Ponton et al. 1999). Studies in adult CI users have generally shown waveforms similar to those recorded with acoustic stimulation, although several studies have reported slightly shorter

Shannon 2007; Wilson and Dorman 2009). Chronic intracochlear electrical stimulation has been shown to affect temporal responsiveness of A1 neurons in deafened cats, with increases in the upper limit of frequency following (Fallon et al. 2007). In our study, strong FFRs were observed in response to both click trains and bursts of SAM noise presented at rates up to 50 Hz. Although PLST in some normal-hearing subjects can exhibit FFRs to higher rate stimuli, including 100 Hz click trains (Nourski et al. 2013a), this was not observed in the present study. The fact that the most posterior region of PLST may not have been covered by the

latencies and smaller N_1 amplitudes in CI users compared to normal-hearing controls (Micco et al. 1995; Ponton et al. 1996; Firszt et al. 2002; Kelly et al. 2005). The response measures in the present study generally showed activity on a comparable time scale with similar waveforms, suggesting a common cortical source. AEP latencies for our subject with a long history of CI use were very similar to those of normal-hearing subjects. This result is consistent with the earlier findings of Pantev et al. (2002), who reported scalp-recorded cortical AEP latencies to be similar when obtained by acoustic and electric stimulation in the same subject before and after implantation. Other scalp EEG studies carried out in CI patients also showed that AEP latencies changed over time, with longer periods of CI use being associated with latencies that more closely resemble normal values (Jordan et al. 1997; Sandmann et al. 2012).

The ECoG provides the advantage of considerably higher spatial and temporal resolution as compared to extracranial recording. The main finding of the present study is the similarity of response properties that characterized noncore auditory cortex on the lateral STG with those previously described in normal-hearing individuals (Brugge et al. 2009; Nourski et al. 2008, 2013a). Thus, while similarities in cortical responses between CI and normal-hearing subjects have been previously reported in extracranial studies, we were able to localize this to a specific auditory cortical area. Taken together, the intracranial and extracranial data suggest that in experienced successful CI users, there may be a relatively normal pattern of activation in the central auditory pathways projecting to noncore auditory cortex on PLST. To facilitate interpretation of surface recordings from a wider population of CI users, plans are underway to follow-up the present study with scalp EEG-based investigations in the same subject.

Spatiotemporal patterns of auditory cortical activity during CI stimulation have been previously studied using recordings from the cortical surface in experimental animals (e.g., Kral et al. 2009). Ponton and Eggermont (2001) compared scalp EEG data from implanted children with direct cortical recordings obtained in deaf white kittens and suggested that the effects of deafness and electrical stimulation of the auditory nerve were similar across the two mammalian species. Invasive electrophysiology studies in experimental animals demonstrate that long duration deafness leads to considerable changes in the organization of the auditory cortex. These changes include decoupling of primary from higher order auditory cortex and cross-modal reorganization (Kral et al. 2002, 2005;

Lomber et al. 2010). The extent of cortical reorganization depends on timing of deafness onset relative to sensitive periods in early auditory cortical development; it is most pronounced in cases of congenital deafness (Kral et al. 2001; Kral and Sharma 2012). Thus, direct comparison of animal studies done in congenitally or neonatally deaf animals with our present findings obtained in a postlingually deaf patient with a long (and successful) history of CI use is not straightforward. We note, however, that chronic electrical stimulation of the auditory nerve, particularly when coupled with behavioral training, can improve temporal processing within the primary auditory cortex of experimentally deafened animals (Beitel et al. 2011; Vollmer and Beitel 2011). The present report is consistent with these animal electrophysiology studies and extends their findings to human nonprimary auditory cortex.

ACKNOWLEDGMENTS

REFERENCES

Abrams DA, Nicol T, Zecker S, Kraus N (2008) Right-hemisphere auditory cortex is dominant for coding syllable patterns in speech. J Neurosci 28:3958–6395

Ahissar E, Ahissar M (2005) Processing of the temporal envelope of speech. In: König R, Heil P, Budinger E, Scheich H (eds) The auditory cortex: a synthesis of human and animal research. Erlbaum, Mahwah, pp 295–314

Ahissar E, Nagarajan S, Ahissar M, Protopapas A, Mahncke H, Merzenich MM (2001) Speech comprehension is correlated with temporal response patterns recorded from auditory cortex. Proc Natl Acad Sci U S A 98:13367–13372

Ashley HL (2000) Cochlear implants in the United Kingdom. Cochlear Implants Int 1:16–17

Avants B, Epstein CL, Gee JC (2006) Geodesic image normalization in the space of diffeomorphisms. In: Mathematical foundations of computational anatomy: geometrical and statistical methods for modelling biological shape variability, October 1 2006, Copenhagen, Denmark. MFCA'06 Workshop Proceedings 125–133

Avants B, Epstein CL, Grossman M, Gee JC (2008) Symmetric diffeomorphic image registration with cross-correlation: evaluat-

ing automated labeling of elderly and neurodegenerative brain. Med Image Analysis 12:26–41

BEITEL RE, VOLLMER M, RAGGIO MW, SCHREINER CE (2011) Behavioral training enhances cortical temporal processing in neonatally deafened juvenile cats. J Neurophysiol 106:944–959

BOOTHROYD A, HANIN L, HNATH T (1985) CUNY laser videodisk of everyday sentences. Speech and Hearing Sciences Research Center, City University of New York, New York

BROWN CJ, ETLER C, HE S, O'BRIEN S, ERENBERG S, KIM JR, DHULDHOYA AN, ABBAS PJ (2008) The electrically evoked auditory change complex: preliminary results from nucleus cochlear implant users. Ear Hear 29:704–717

BRUGGE JF, NOURSKI KV, OYA H, KAWASAKI H, REALE RA, HOWARD MA (2008A) Representation of sinusoidal amplitude modulated noise within the primary auditory (core) cortex of human. Society for Neuroscience 38th Annual Meeting. November 15–19, 2008, Washington, DC Program No. 566.6. 2008 Abstract Viewer/Itinerary Planner. Washington, DC: Society for Neuroscience, 2008. Online

BRUGGE JF, VOLKOV IO, OYA H, KAWASAKI H, REALE RA, FENOY A, STEINSCHNEIDER M, HOWARD MA III (2008B) Functional localization of auditory cortical fields of human: click-train stimulation. Hear Res 238:12–24

BRUGGE JF, NOURSKI KV, OYA H, REALE RA, KAWASAKI H, STEINSCHNEIDER M, HOWARD MA III (2009) Coding of repetitive transients by auditory cortex of Heschl's gyrus of human. J Neurophysiol 102:2358–2374

CERVENKA MC, NAGLE S, BOATMAN-REICH D (2011) Cortical high-gamma responses in auditory processing. Am J Audiol 20:171–180

CRONE NE, BOATMAN D, GORDON B, HAO L (2001) Induced electrocorticographic gamma activity during auditory perception. Clin Neurophysiol 112:565–582

EDWARDS E, SOLTANI M, KIM W, DALAL SS, NAGARAJAN SS, BERGER MS, KNIGHT RT (2009) Comparison of time-frequency responses and the event-related potential to auditory speech stimuli in human cortex. J Neurophysiol 102:377–386

ENGEL AK, MOLL CK, FRIED I, OJEMANN GA (2005) Invasive recordings from the human brain: clinical insights and beyond. Nat Rev Neurosci 6:35–47

FALLON J, IRVINE D, COCO A, DONLEY L, MILLARD R, SHEPHERD R (2007) Cochlear implantation influences the temporal responsiveness of the primary auditory cortex in the deafened cat. Assoc. Res. Otolaryngol. 2007 MidWinter Meeting. February 10–15, 2007, Denver, CO. Assoc. Res. Otolaryngol Abs: 507

FALLON JB, IRVINE DR, SHEPHERD RK (2009) Neural prostheses and brain plasticity. J Neural Eng 6:065008

FAYAD JN, LINTHICUM FH (2006) Multichannel cochlear implants: relation of histopathology to performance. Laryngoscope 116:1310–1320

FIRSZT JB, CHAMBERS RD, KRAUS N, REEDER RM (2002) Neurophysiology of cochlear implant users I: effects of stimulus current level and electrode site on the electrical ABR, MLR and N1-P2 response. Ear Hear 23:502–515

FU QJ (2002) Temporal processing and speech recognition in cochlear implant users. Neuroreport 13:1635–1639

GILLEY PM, SHARMA A, DORMAN M, FINLEY CC, PANCH AS, MARTIN K (2006) Minimization of cochlear implant stimulus artifact in cortical auditory evoked potentials. Clin Neurophysiol 117:1949–56

GIRAUD AL, TRUY E, FRACKOWIAK R (2001) Imaging plasticity in cochlear implant patients. Audiol Neurootol 6:381–393

GREENLEE JD, JACKSON AW, CHEN F, LARSON CR, OYA H, KAWASAKI H, CHEN H, HOWARD MA III (2011) Human auditory cortical activation during self-vocalization. PLoS ONE 6:e14744

GREENLEE J, BEHROOZMAND R, ETLER C, NOURSKI K, OYA H, KAWASAKI H, HOWARD M (2012) Auditory cortical ECoG findings in a bilateral cochlear implant user during self-vocalization. 4th International Conference on Auditory Cortex. August 31–September 3, 2012, Lausanne, Switzerland, p 142

HIRSH L, DAVIS H, SILVERMAN S, REYNOLDS E, ELDERT E, BENSON R (1952) Development of materials for speech audiometry. J Speech Hear Disord 17:321–337

HOWARD MA, VOLKOV IO, MIRSKY R, GARELL PC, NOH MD, GRANNER M, DAMASIO H, STEINSCHNEIDER M, REALE RA, HIND JE, BRUGGE JF (2000) Auditory cortex on the human posterior superior temporal gyrus. J Comp Neurol 416:79–92

HOWARD MA, NOURSKI KV, BRUGGE JF (2012) Invasive research methods. In: Fay RR, Popper AN (eds) Springer handbook of auditory research—human auditory cortex. Springer, New York, pp 39–67

IRVINE DR, FALLON JB, KAMKE MR (2006) Plasticity in the adult central auditory system. Acoust Aust 34:13–17

JORDAN K, SCHMIDT A, PLOTZ K, VON SPECHT H, BEGALL K, ROTH N, SCHEICH H (1997) Auditory event-related potentials in post- and prelingually deaf cochlear implant recipients. Am J Otol 18:S116–S117

KELLY AS, PURDY SC, THORNE PR (2005) Electrophysiological and speech perception measures of auditory processing in experienced adult cochlear implant users. Clin Neurophysiol 116:1235–1246

KLINKE R, KRAL A, HEID S, TILLEIN J, HARTMANN R (1999) Recruitment of the auditory cortex in congenitally deaf cats by long-term cochlear electrostimulation. Science 285:1729–1733

KLINKE R, HARTMANN R, HEID S, TILLEIN J, KRAL A (2001) Plastic changes in the auditory cortex of congenitally deaf cats following cochlear implantation. Audiol Neurootol 6:203–206

KRAL A, SHARMA A (2012) Developmental neuroplasticity after cochlear implantation. Trends Neurosci 35:111–122

KRAL A, TILLEIN J (2006) Brain plasticity under cochlear implant stimulation. Adv Otorhinolaryngol 64:89–108

KRAL A, HARTMANN R, TILLEIN J, HEID S, KLINKE R (2001) Delayed maturation and sensitive periods in the auditory cortex. Audiol Neurootol 6:346–362

KRAL A, HARTMANN R, TILLEIN J, HEID S, KLINKE R (2002) Hearing after congenital deafness: central auditory plasticity and sensory deprivation. Cereb Cortex 12:797–807

KRAL A, TILLEIN J, HEID S, HARTMANN R, KLINKE R (2005) Postnatal cortical development in congenital auditory deprivation. Cereb Cortex 15:552–562

KRAL A, TILLEIN J, HUBKA P, SCHIEMANN D, HEID S, HARTMANN R, ENGEL AK (2009) Spatiotemporal patterns of cortical activity with bilateral cochlear implants in congenital deafness. J Neurosci 29:811–827

KRUEGER B, JOSEPH G, ROST U, STRAUSS-SCHIER A, LENARZ T, BUECHNER A (2008) Performance groups in adult cochlear implant users: speech perception results from 1984 until today. Otol Neurotol 29:509–512

LAW SK, NUNEZ PL, WIJESINGHE RS (1993) High-resolution EEG using spline generated surface Laplacians on spherical and ellipsoidal surfaces. IEEE Trans Biomed Eng 40:145–153

LINTHICUM FH JR, ANDERSON W (1991) Cochlear implantation of totally deaf ears. Histologic evaluation of candidacy. Acta Otolaryngol 111:327–31

LINTHICUM FH JR, FAYAD J, OTTO SR, GALEY FR, HOUSE WF (1991) Cochlear implant histopathology. Am J Otol 12:245–311

LOMBER SG, MEREDITH MA, KRAL A (2010) Cross-modal plasticity in specific auditory cortices underlies visual compensations in the deaf. Nat Neurosci 13:1421–1427

MARTIN BA (2007) Can the acoustic change complex be recorded in an individual with a cochlear implant? Separating neural responses from cochlear implant artifact. J Am Acad Audiol 18:126–140

McKay CM, McDermott HJ, Clark GM (1994) Pitch percepts associated with amplitude-modulated current pulse trains in cochlear implantees. J Acoust Soc Am 96:2664–2673

Micco AG, Kraus N, Koch DB, McGee TJ, Carrell TD, Sharma A, Nicol T, Wiet RJ (1995) Speeech evoked cognitive p300 potentials in cochlear implant recipients. Am J Otol 16:514–520

Millman RE, Prendergast G, Hymers M, Green GG (2013) Representations of the temporal envelope of sounds in human auditory cortex: can the results from invasive intracortical "depth" electrode recordings be replicated using non-invasive MEG "virtual electrodes"? Neuroimage 64:185–196

Moore DR, Shannon RV (2009) Beyond cochlear implants: awakening the deafened brain. Nat Neurosci 12:686–691

Näätänen R, Picton T (1987) The N1 wave of the human electric and magnetic response to sound: a review and an analysis of the component structure. Psychophysiology 24:375–425

Nichols TE, Holmes AP (2002) Nonparametric permutation tests for functional neuroimaging: a primer with examples. Hum Brain Mapp 15:1–25

NIDCD (2011) NIDCD fact sheet: cochlear implants. NIH Publication No. 11-4798

NIH (1995) Cochlear implants in adults and children. NIH Consensus Statement 13:1–30

Nilsson M, Soli SD, Sullivan JA (1994) Development of the hearing in noise test for the measurement of speech reception thresholds in quiet and noise. J Acoust Soc Am 95:1085–1099

Nourski KV, Brugge JF (2011) Representation of temporal sound features in the human auditory cortex. Rev Neurosci 22:187–203

Nourski KV, Oya H, Kawasaki H, Reale RA, Howard MA, Brugge JF (2008) Representation of time-compressed speech in human auditory cortex. Society for Neuroscience 38th Annual Meeting. November 15–19, 2008, Washington, DC Program No. 566.5. 2008 Abstract Viewer/Itinerary Planner. Washington, DC: Society for Neuroscience, 2008. Online

Nourski KV, Reale RA, Oya H, Kawasaki H, Kovach CK, Chen H, Howard MA III, Brugge JF (2009) Temporal envelope of time-compressed speech represented in the human auditory cortex. J Neurosci 29:15564–15574

Nourski K, Brugge J, Reale R, Oya H, Kawasaki H, Howard M (2010) Electrophysiological study of responses to amplitude-modulated noise within human lateral superior temporal gyrus. Assoc. Res. Otolaryngol. 2010 MidWinter Meeting. February 6–10, 2010, Anaheim, CA. Assoc Res Otolaryngol Abs: 301

Nourski K, Etler C, Brugge J, Oya H, Kawasaki H, Abbas P, Brown C, Howard M (2012) Direct recordings from the auditory cortex in a bilateral cochlear implant user. 4th International Conference on Auditory Cortex. August 31–September 3, 2012, Lausanne, Switzerland, p 140

Nourski KV, Brugge JF, Reale RA, Kovach CK, Kawasaki H, Oya H, Jenison RL, Howard M (2013a) Coding of repetitive transients by auditory cortex on posterolateral superior temporal gyrus in humans: an intracranial electrophysiology study. J Neurophysiol 109:1283–1295

Nourski KV, Steinschneider M, Oya H, Kawasaki H, Jones RD, Howard MA III (2013b) Spectral organization of the human lateral superior temporal gyrus revealed by intracranial recordings. Cereb Cortex. doi:10.1093/cercor/bhs314

Nunez P (1981) Electric fields of the brain. Oxford University Press, New York

Nunez PL, Pilgreen KL (1991) The spline-Laplacian in clinical neurophysiology: a method to improve EEG spatial resolution. J Clin Neurophysiol 8:397–413

Oya H, Kawasaki H, Howard MA III, Adolphs R (2002) Electrophysiological responses in the human amygdala discriminate emotion categories of complex visual stimuli. J Neurosci 22:9502–9512

Pantev C, Ross B, Wollbrink A, Riebandt M, Delank KW, Seifert E, Lamprecht-Dinnesen A (2002) Acoustically and electrically evoked responses of the human cortex before and after cochlear implantation. Hear Res 171:191–195

Perrin F, Pernier J, Bertrand O, Giard MH, Echallier JF (1987) Mapping of scalp potentials by surface spline interpolation. Electroencephalogr Clin Neurophysiol 66:75–81

Ponton CW, Eggermont JJ (2001) Of kittens and kids: altered cortical maturation following profound deafness and cochlear implant use. Audiol Neurootol 6:363–380

Ponton CW, Don M, Eggermont JJ, Waring MD, Masuda A (1996) Maturation of human cortical auditory function: differences between normal-hearing children and children with cochlear implants. Ear Hear 17:430–437

Ponton CW, Moore JK, Eggermont JJ (1999) Prolonged deafness limits auditory system developmental plasticity: evidence from an evoked potentials study in children with cochlear implants. Scand Audiol Suppl 51:13–22

Reale RA, Calvert GA, Thesen T, Jenison RL, Kawasaki H, Oya H, Howard MA, Brugge JF (2007) Auditory–visual processing represented in the human superior temporal gyrus. Neuroscience 145:162–184

Rhone A, Oya H, McMurray B, Reale R, Etler C, Nourski K, Kawasaki H, Howard M (2012) Auditory, visual, and audiovisual speech responses recorded directly from the temporal lobe of a bilateral cochlear implant user. 4th International Conference on Auditory Cortex. August 31–September 3, 2012, Lausanne, Switzerland. p 141

Sandmann P, Plotz K, Volpert S, Siegel M, Schoenfield R, Debener S (2012) Dynamics of cortical plasticity in cochlear-implant users: a prospective longitudinal study. 4th International Conference on Auditory Cortex. August 31–September 3, 2012, Lausanne, Switzerland. p 117

Shannon RV (2007) Understanding hearing through deafness. Proc Nat Acad Sci U S A 104:6883–6884

Shepherd RK, Hardie NA (2001) Deafness-induced changes in the auditory pathway: implications for cochlear implants. Audiol Neurootol 6:305–318

Singh S, Liasis A, Rajput K, Luxon L (2004) Short report: methodological considerations in recording mismatch negativity in cochlear implant patients. Cochlear Implants Int 5:76–80

Steinschneider M, Nourski KV, Kawasaki H, Oya H, Brugge JF, Howard MA III (2011) Intracranial study of speech-elicited activity on the human posterolateral superior temporal gyrus. Cereb Cortex 21:2332–2347

Tillman TW, Carhart R (1966) An expanded test for speech discrimination utilizing CNC monosyllabic words. Northwestern University auditory test No. 6. USAF School of Aerospace Medicine, Brooks Air Force Base, TX

Ventry IM, Weinstein BE (1982) The hearing handicap inventory for the elderly: a new tool. Ear Hear 3:128–134

Viola FC, De Vos M, Hine J, Sandmann P, Bleeck S, Eyles J, Debener S (2012) Semi-automatic attenuation of cochlear implant artifacts for the evaluation of late auditory evoked potentials. Hear Res 284:6–15

Vollmer M, Beitel RE (2011) Behavioral training restores temporal processing in auditory cortex of long-deaf cats. J Neurophysiol 106:2423–2436

Wilson BS, Dorman MF (2009) The design of cochlear implants. In: Niparko JK (ed) Cochlear implants: principles & practices. Lippincott Williams & Wilkins, Philadelphia, pp 95–135